

# Photographic feature: Revealing millimetre-scale ground movements in London using SqueeSAR™

Christine A. Bischoff, Richard C. Ghail, Philippa J. Mason, Alessandro Ferretti and John A. Davis

Quarterly Journal of Engineering Geology and Hydrogeology

## Abstract

A series of illustrated examples is presented here to demonstrate the capabilities of ground-level monitoring using InSAR (interferometric synthetic aperture radar). Greater London is an ideal area to demonstrate and validate measurements derived using InSAR; its continuous urban fabric and the regular acquisition of SAR images from high-resolution sensors, such as TerraSAR-X, allows detection and monitoring of over 1.7 million measurement points with millimetre-scale accuracy. The results, some of which are shown here, reveal fascinating spatial and temporal patterns of ground motion across London and demonstrate the benefit of using high-resolution InSAR technologies in engineering applications. Interpreting the motion patterns can be challenging, however, owing to their complex and sometimes mysterious causes; we therefore welcome any assistance in doing so and we hope this photographic feature serves to trigger interest.

## Introduction

InSAR (interferometric synthetic aperture radar) is a remote sensing tool that provides reliable ground surface displacement measurements. Greater London is an ideal area to demonstrate this technique's capabilities, as is shown in the following examples. London's continuous urban fabric as well as regular acquisition of SAR images from high-resolution sensors such as TerraSAR-X allow monitoring over 1.7 million measurement points with millimetre-scale accuracy, offering a unique way to detect the millimetre-scale regional movements originating from civil engineering projects across London.

The processed data results presented here represent ground motion measured in the line of sight (LOS), without any interpretation, and are presented as average LOS ground velocity (in mm a<sup>-1</sup>) or cumulative displacement (in mm). They were processed using an advanced multi-interferogram technique called SqueeSAR™ (Ferretti et al. 2011) at TRE ALTAMIRA, Milan, Italy. A variety of multi-interferogram techniques have been developed in the past 20 years, the majority of which belong to one of two families of algorithms (Ferretti 2014): permanent scatterer interferometry (PSI; Ferretti et al. 2001) and small baseline subset (SBAS; Berardino et al. 2002). A review of multi-interferogram techniques has been given by Osmanoglu et al. (2016). The SqueeSAR™ method combines elements from both SBAS and PSI techniques, thereby achieving a high measurement point density over areas characterized by distributed scatterers or DS (identified by SBAS-type algorithms), while preserving the information provided by point-wise (or permanent) scatterers (PS) used in PSI. A detailed description and explanation of the SqueeSAR™ technique has been given by Ferretti et al. (2011).

The majority of measurement points shown in the following supporting figures are permanent scatterers. These are ground objects that reflect radar waves in a way that is stable over time; that is, the object's radar return does not lose coherence (Ferretti et al. 2001). Amplitude and phase information are recorded for each radar image; any change in or movement of the PS position will

result in a phase shift of the radar return between an image acquired before and one acquired after the movement (Ferretti 2014). After filtering out noise and topographic and atmospheric effects, this phase shift can be translated into a displacement in the LOS of the sensor, providing measurements of ground movement at millimetre-scale accuracy (Ferretti et al. 2007).

The ground motion data presented here are derived from a fixed set of 150 images covering the same region of the Greater London area, acquired by an X-band (wavelength 3.1 mm) sensor mounted on the TerraSAR-X satellite, in regular, usually 11 day, intervals between 1 May 2011 and 28 April 2017. The measurements have millimetre-scale accuracy owing to the high number of images (150) and the long timespan covered (6 years). The dataset contains, on average, 1482 measurement points per km<sup>2</sup> in an area of over 650 km<sup>2</sup>. All displacement values referred to in this paper are in the LOS of the sensor, which in this case means at an incidence angle of 37.33°. Figures 1–5 show surface displacement over a range of construction sites.

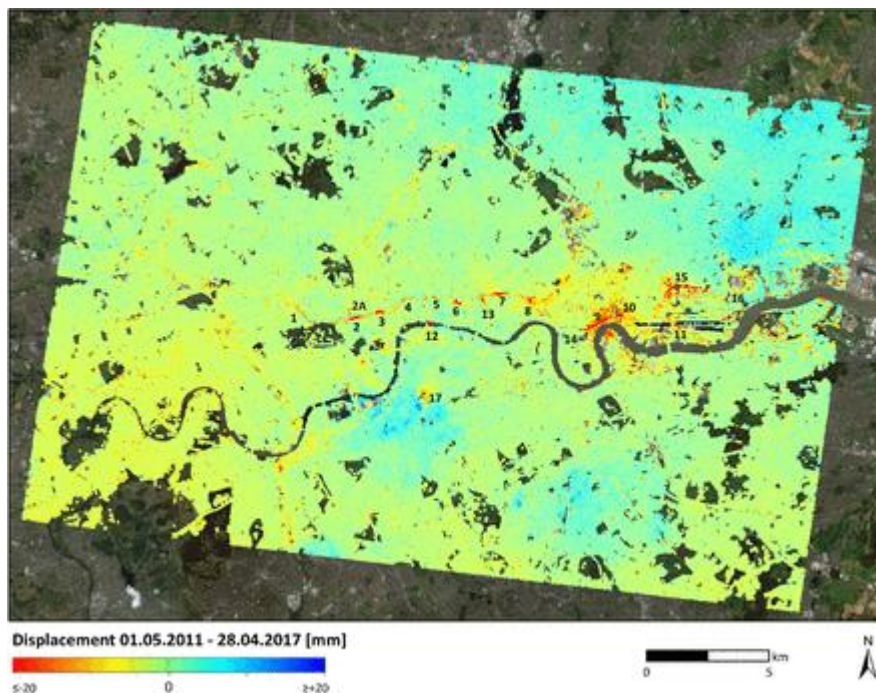


**Fig. 1.** Total displacement in the line of sight (LOS), in millimetres, of 1 788 295 permanent scatterers (PS) and distributed scatterers (DS) based on 150 TerraSAR-X scenes acquired between 1 May 2011 and 28 April 2017. The displacement patterns show that, in general, there is little ground movement across London (pale green colours indicate 0 mm) but there are a number of noticeable areas of significant movement, both up and down. The most obvious ground movements include the meandering pattern of settlement associated with the east–west route of the Crossrail project. There are also subtle patterns of uplift to the north and south of the Thames; these are thought to be neo-tectonic effects. Features related to Crossrail: 1, Paddington; 2, Bond Street (Fig. 3); 3, Tottenham Court; 4, Fisher St Crossover (Fig. 2); 5, Farringdon; 6, Liverpool St; 7, Whitechapel and Vallance Rd crossover; 8, Stepney Green Junction; 9, dewatering for cross passages (Fig. 5); 10, Limmo shaft dewatering (Fig. 6); 11, Connaught Tunnel dewatering. Other features of interest: 2A, Bond St Station upgrade (Fig. 4); 12, Blackfriars Bridge (Fig. 8); 13, a cable tunnel; 14, the effects of extensive dewatering at Canary Wharf are not seen, because pumping started prior to 2011 and had not ceased at the time of writing; 15, Lee Tunnel and a drift-filled hollow; 16, Lee Tunnel shafts at Beckton; 17, Northern Line Extension dewatering (Fig. 7).

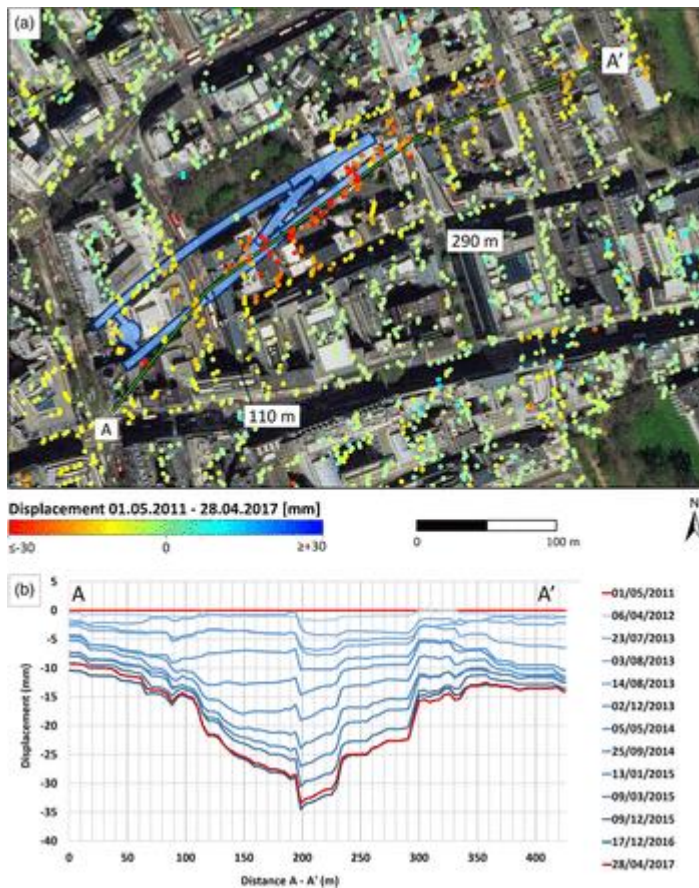


**Fig. 2.** Fisher Street crossover. (a) Map view of the area above the Crossrail Fisher Street crossover cavern. An outline of the tunnel location is shown in blue. (b) Profile from A to A' along the tunnel location, which was constructed using the mean of PS displacement measurements within  $40 \times 40$  m windows centred on nodes spaced every 10 m along the profile line. The profile shows that the displacement measured by PS is 35 mm and variable along the profile.

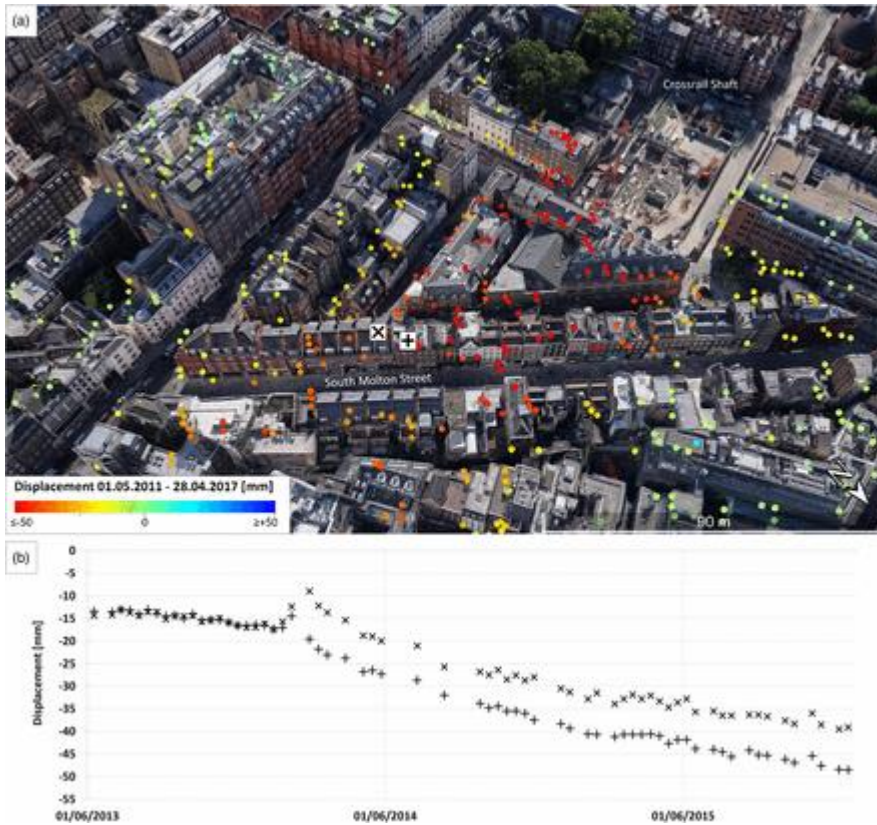


**Fig. 3.** Bond Street Station. (a) A 3D view, facing SW, of the PS measurements in the area around the western end of the mined Crossrail Bond Street Station; the Crossrail Western Ticket Hall box is in the top right corner. (b) Time series of two PS located on separate but directly adjacent buildings in South Molton Street, indicated in (a). As can be seen from the graphs in (b), only the building to the south is affected by an uplift of 10 mm, which eventually causes about 10 mm difference in the final settlement. The uplift is most probably caused by Crossrail compensation grouting.

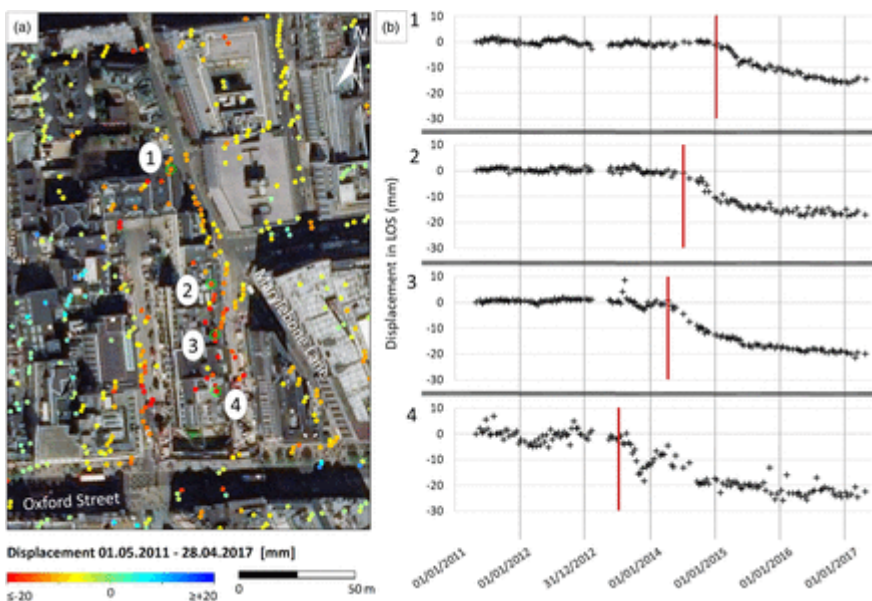


**Fig. 4.** Bond Street Station Upgrade. (a) Response of buildings to the tunnelling works for London Underground's recent Bond St Station upgrade. The data show settlement of 20 mm just north of Oxford Street. (b) Time series of four PS, with their location indicated by green circles in (a). The red

bars indicate the start of settlement recorded by these four PS, progressing from south to north. Time series 4 furthermore shows a sudden drop and direct recovery of 15 mm, a pattern that is also visible and synchronous, although less pronounced, in time series 3.

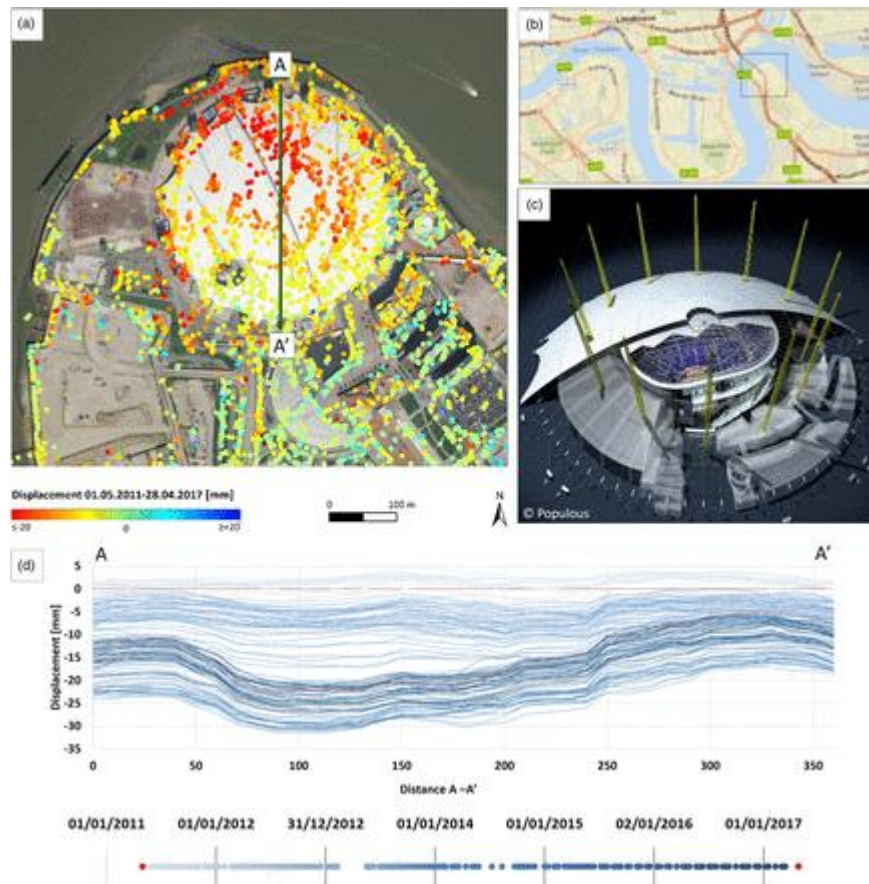


**Fig. 5.** O2 Arena. (a) PS measurements over and around the O2 Arena during Crossrail dewatering works, located in East London, as shown in (b). The O2 Arena's roof is actually a non-metallic 'tent' as shown in (c), which means that radar beam can pass through it and so the PS represent movement of the structures underneath the tent rather than the tent itself. (d) Cross-section across the O2 Arena, A–A', constructed using the mean of PS measurements within 50 × 50 m windows centred on nodes spaced every 10 m along the section. The graph below the cross-section indicates which dates are represented by which colour. The cross-section shows that the area was affected mainly by contiguous settlement and rebound related to dewatering; however, during winter 2013–2014, there was a 10 mm greater settlement in the northern half of the section, a difference that persists in the ensuing ground rebound. (a) also shows that river embankments north of the O2 Arena are affected by 1–2 cm of settlement between 2011 and 2017.

## Background on radar interferometry

The remote sensing technique generally referred to as InSAR was initially applied to large-scale natural movements such as earthquakes (Massonnet et al. 1993), but it has since developed into a monitoring technique for millimetre-scale movements caused by human activity such as oil reservoir elevation changes (Ferretti 2014), but also for infrastructure. Common civil engineering applications include monitoring of tunnels (Barla et al. 2016), bridges (Lazecky et al. 2015), single structures (Giannico et al. 2012) and general urban subsidence (Osmanoğlu et al. 2011). The examples

presented in this paper focus principally on measurements of ground movement associated with recent tunnelling activities in the Greater London area.

InSAR allows measurement of ground deformation by detecting the phase differences between at least two SAR images (Goldstein et al. 1988; Rosen et al. 2000). A tutorial by Moreira et al. (2013) gives a comprehensive introduction to the basic concepts of synthetic aperture radar, and Osmanoğlu et al. (2016) reviewed the advantages and limitations of several InSAR processing algorithms.

Infrastructure monitoring is, in general, performed using permanent scatterer interferometry (PSI), a technique that mitigates the limitations of conventional InSAR; most importantly, the artefacts introduced by the Earth's atmosphere (Ferretti et al. 2001; Barla et al. 2016). Although SqueeSAR™ detects both distributed and permanent scatterers, in the case of urban areas such as London the majority of scatterers are permanent. Rather than producing an interferogram based on just two radar images, multi-interferogram techniques exploit a stack of several SAR images. Objects on the ground that do not change the way they reflect the radar signal over time (point-wise targets, such as building rooftops, facades and road surfaces) are identified as permanent scatterers (Ferretti et al. 2001). This allows a better filtering of the atmospheric phase contribution and results in a set of measurement points (permanent scatterers) with an associated time series corresponding to the acquisition dates of the images in the stack.

## **Anomalies in London's geology highlighted by construction-related ground movement**

The basement geology under London is overlain by a comparatively thin (c. 100 m) layer of Chalk, followed by Paleogene and Quaternary sediments, including the Thanet Sand, London Clay and River Terrace Deposits (Aldiss 2014). A summary of the stratigraphy found under Central London and adjacent areas has been given by Royse et al. (2012) and a detailed guide has been provided by Ellison et al. (2004) and in the British Geological Survey report authored by Aldiss (2014).

The thickness and extent of the strata are highly variable across the Greater London area; such variations are the result of its complex tectonic history (Royse et al. 2012). Most Paleogene strata are laterally discontinuous, reflecting the highly variable palaeo-environments of their deposition: marine, deltaic, estuarine, terrestrial and glacial–fluvial, with evidence of prolonged periods of erosion (Aldiss 2014).

The surface ground movement caused by large-scale civil engineering projects, such as the Crossrail tunnels, is closely linked to the local geology. The London Clay Formation is generally considered to be well suited to tunnelling (Black 2017), but the stratigraphy in London contains several units that present a variety of challenges to geotechnical engineers. Davis (2016) published a practical review of London's geology from a geotechnical engineer's perspective and pointed out a number of potential problems for tunnelling within the different stratigraphic layers, such as hard pans in the Lambeth Group and buried hollows (Banks et al. 2015). Arguably most challenging is the Lambeth Group, because its properties are highly variable, both laterally and vertically.

A key problem for geotechnical engineers is that these challenging ground conditions often occur unexpectedly and at scales too small to be represented in published geological models (Aldiss 2013). However, the ground movement originating from subsurface construction projects, especially from dewatering and tunnelling itself, is detectable with PSInSAR. The surface expression of these two mechanisms is, among many other factors, dependent on the local geology. PSInSAR data uniquely

highlight millimetric differences in ground deformation over a wide area and so constrain likely locations of geological discontinuities and anomalies, as demonstrated in Figures 1–7.

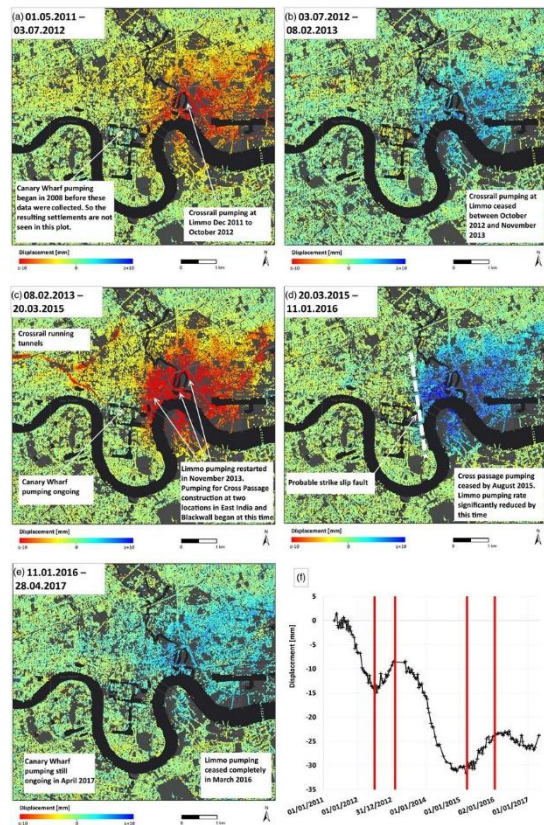


**Fig. 6.** Limmo dewatering. (a)–(e) show the impact as measured by InSAR of the dewatering necessary for Crossrail's construction in East London around the Limmo peninsula. The TerraSAR-X data were partitioned into five time periods, defined by the response to dewatering; the cut-off times are indicated by the red bars in (f), which shows a representative time series near the Limmo Peninsula. The maps show the total displacement that took place between the dates indicated at the top, therefore the settlement directly caused by Crossrail tunnels for example is visible only in (c). The precision of the measurements calculated in the 6 month periods is lower with respect to the entire monitored period.

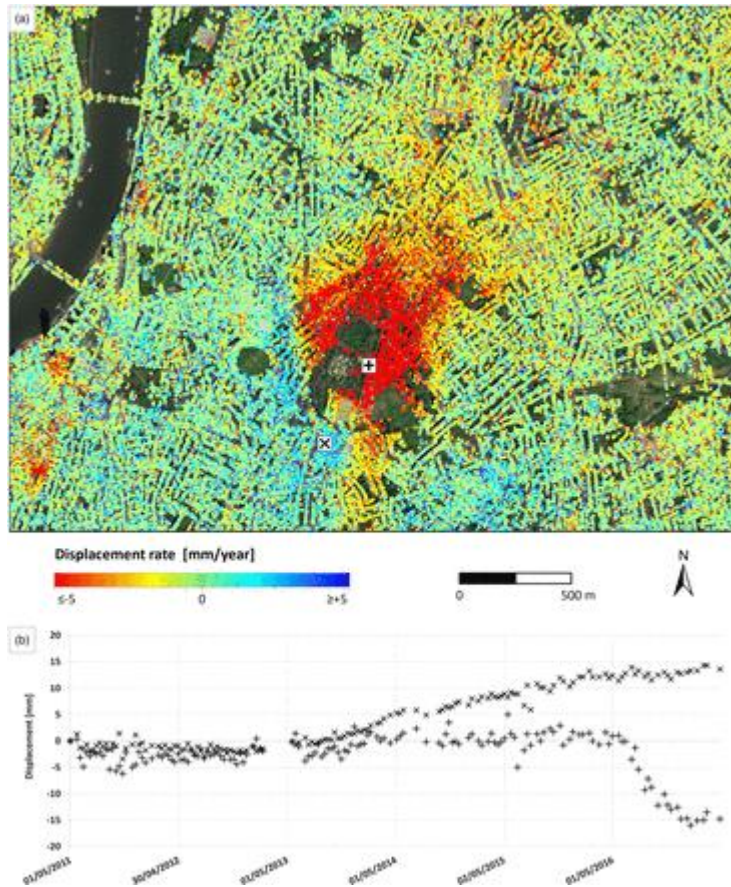


**Fig. 7.** Northern Line Extension. (a) Map of the area around Kennington Park and the Oval, which highlights the impact of dewatering necessary for the construction of some of the subsurface Northern Line Extension works. The colour represents the average annual displacement between 1 January 2016 and 28 April 2017. The time series of two PS points are shown in (b) with their locations indicated in (a). Both (a) and (b) indicate a linear north–south disparity in this area. The time series of the southern PS (diagonal cross) indicates that this area has been affected by continuous uplift since the end of 2013, a trend that is not seen on the northern side, as shown by the time series of the more northern PS (upright cross). However, since dewatering started in 2016, its impact is visible only on the northern side and the uplift trend in the time series of the southern PS (diagonal cross) shown in (b) seems unaffected.

### Expected and detected ground movement related to tunnelling in London

The ground response to tunnelling-related grouting and settlement troughs are local (tens of metres extent) and their short-term behaviour is well understood when compared with long-term associations (Jurečič et al. 2013; Farrell 2015; Hill & Stärk 2015). A Crossrail case study at Kempton Court, Whitechapel, showed that the short-term settlement trough conformed to the predicted form, whereas the long-term settlement trough was wider than expected (Hill & Stärk 2016). Evidently, the empirical based methods currently used to predict long-term settlement troughs, especially towards the edges of the trough, can be improved (Wongsaroj et al. 2007, 2013; Hill & Stärk 2015; Hover et al. 2015). For a better prediction model, accurate measurements of the long-term development of existing settlement troughs are essential, which is an ideal application for PSInSAR in an urban environment such as London. The TerraSAR-X data presented in this paper reveal a complex pattern of settlement trough extent and magnitude, as shown in Figures 1 and 2,

which is often influenced by a combination of factors including local geology, mitigation measures, tunnelling method and dewatering.

In contrast to the local impact of tunnel excavation and grouting shown in Figures 3 and 4, dewatering for London's Crossrail has caused regional ground deformation over a significantly wider area of several square kilometres, which makes it difficult to monitor. The majority of studies published on the impact of Crossrail dewatering are based on readings from a grid of piezometers, as well as ground-based monitoring data in relatively close proximity to the construction sites (Lawrence et al. 2016, 2018). However, the associated regional ground movement was so far unknown, and is shown in Figures 5 and 6. Similarly, ground movement caused by dewatering for the Northern Line Extension is shown in Figure 7.

## PSInSAR as a potential monitoring tool for civil engineering projects

It is clear from the examples shown in this paper that the civil engineering projects taking place across the capital cause displacement measurable with PSInSAR. This is not limited to subsurface construction, and large structures, such as Blackfriars Bridge, clearly experience movement (presumably settlement), as shown in Figure 8. The examples also highlight the complexities involved in interpreting InSAR data correctly to gain valid information. As shown in Figure 6, subsidence and subsequent ground rebound demonstrate that the whole time series of the data needs to be considered rather than just looking at average LOS velocity (mm a<sup>-1</sup>) or cumulative displacement. Furthermore, it is important to consider where a permanent scatterer is actually located on the ground, as shown in Figure 7 where some permanent scatterers represent structures underneath rather than on top of the O2's domed canopy roof.

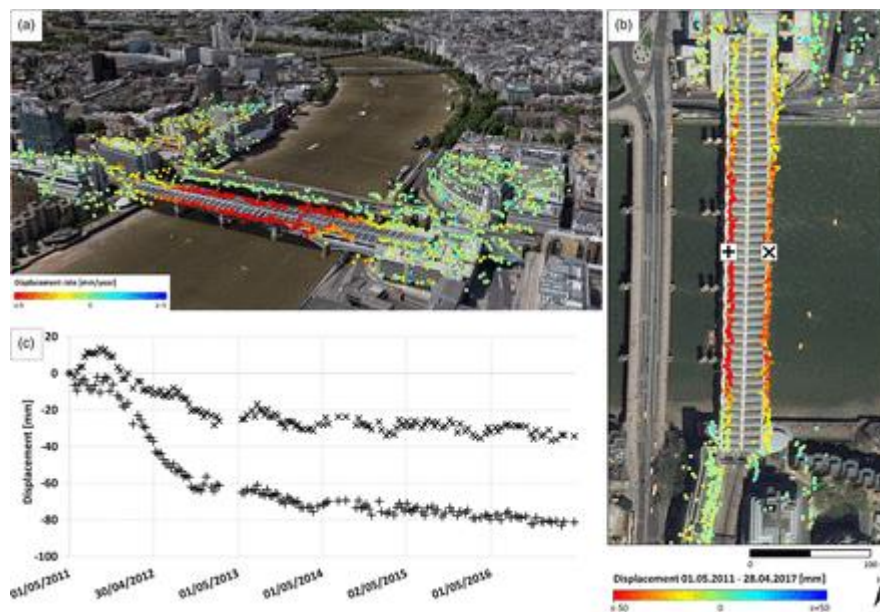


**Fig. 8.** Blackfriars Bridge. (a) A 3D image of the bridge, in Central London, to illustrate the settlement during work to reconstruct Blackfriars station. (b) Map view of the bridge and the location of two PS located on the central eastern and western side of the bridge, whose time series is shown in (c). There is a pronounced difference in total displacement magnitude between the eastern and the western side. The majority of PS on the eastern side of the bridge show settlement between 25 and 45 mm, whereas the PS on the western side move at a more varying rate, with a total settlement of up to 80 mm in the centre of the bridge. We have interpreted this differential settlement as related

to the addition of three steel arched ribs on the bridge's western side, compared with only one steel arched rib on the eastern side (Baecke 2016).

Even so, this TerraSAR-X dataset has considerable and unique advantages over other monitoring techniques, not least the high measurement point density over a wide area and, without the need to install any equipment on the ground, a measurement accuracy of a few millimetres, and a bimonthly measurement frequency for each point over several years. No conventional ground-level measurement technique can achieve such attributes in a timely way without significant costs. Nor can a conventional method achieve such measurements retrospectively to establish a pre-engineering works baseline. This approach (i.e. high-resolution SAR used with an advanced PSI algorithm such as SqueeSAR™) presents a powerful and perhaps unique way to achieve cost-effective, high-precision monitoring of ground movement, over a wide area, both retrospectively and going forward; we suggest it should become a matter of best practice for all ground engineering works.

## **Acknowledgements**

The background maps in Figures 1, 2, 4, 5a, 7, 8b are credited to Esri, Digital Globe, GeoEye, Earthstar Geographics, CNES/Airbus DS, USDA, USGS, AeroGRID, IGN, GIS User Community. The background map in Figure 5(b) is credited to Esri, HERE, Garmin, USGS, Intermap, INCREMENT P, NRCan, Esri Japan, METI, Esri China (Hong Kong), Esri Korea, Esri (Thailand), NGCC, (c) OpenStreetMap contributors, GIS User Community. The background maps in Figures 3 and 8a are credited to Google Earth, 2018.

## **Funding**

This work was funded by the Engineering and Physical Sciences Research Council grant reference: EP/L016826/1.

## **References**

Aldiss, D.T. 2013. Under-representation of faults on geological maps of the London region: reasons, consequences and solutions. *Proceedings of the Geologists' Association*, 124, 929–945

Aldiss, D.T. 2014. *The Stratigraphical Framework for the Palaeogene Successions of the London Basin*, UK. British Geological Survey, Open Report, OR/14/008

Baecke, E. 2016. Reconstruction of Blackfriars railway bridge, London, UK. *Proceedings of the Institution of Civil Engineers – Bridge Engineering*, 169, 191–202

Banks, V.J., Bricker, S.H., Royse, K.R. & Collins, P.E.F. 2015. Anomalous buried hollows in London: development of a hazard susceptibility map. *Quarterly Journal of Engineering Geology and Hydrogeology*, 48, 55–70

Barla, G., Tamburini, A., Del Conte, S. & Giannico, C. 2016. InSAR monitoring of tunnel induced ground movements. *Geomechanik und Tunnelbau*, 9, 15–22

Berardino, P., Mora, O., Lanari, R., Mallorqui, J.J. & Sansosti, E. 2002. A new algorithm for monitoring localized deformation phenomena based on small baseline differential SAR interferograms. *IEEE International Geoscience and Remote Sensing Symposium*, 2, 1237–1239

Black, M. 2017. Crossrail project: managing geotechnical risk on London's Elizabeth line. *Proceedings of the Institution of Civil Engineers – Civil Engineering*, 170, 23–30

Davis, J. 2016. A geology of London for tunnellers and engineers. In: Black, M. (ed.) *Crossrail Project: Infrastructure Design and Construction*. ICE Publishing, London, 447–459

Ellison, R.A., Woods, M.A., Allen, D.J., Forster, A., Pharaoh, T.C. & King, C. 2004. *Geology of London: Special Memoir for 1:50000 Geological Sheets 256 (North London), 257 (Romford), 270 (South London), and 271 (Dartford) (England and Wales)*. British Geological Survey, Nottingham

Farrell, R.P. 2015. Tunnelling and compensation grouting at Bond Street, London. *Proceedings of the Institution of Civil Engineers – Geotechnical Engineering*, 168, 471–482

Ferretti, A. 2014. *Satellite InSAR Data – Reservoir Monitoring from Space*. EAGE Publications, Houten

Ferretti, A., Prati, C. & Rocca, F. 2001. Permanent scatterers in SAR interferometry. *IEEE Transactions on Geoscience and Remote Sensing*, 39, 8–20

Ferretti, A., Savio, G. et al. 2007. Submillimeter accuracy of InSAR time series: Experimental validation. *IEEE Transactions on Geoscience and Remote Sensing*, 45, 1142–1153

Ferretti, A., Fumagalli, A., Novali, F., Prati, C., Rocca, F. & Rucci, A. 2011. A new algorithm for processing interferometric data-stacks: SqueeSAR. *IEEE Transactions on Geoscience and Remote Sensing*, 49, 3460–3470

Giannico, C., Ferretti, A., Jurina, L. & Ricci, M. 2012. Application of satellite radar interferometry for structural damage assessment and monitoring. In: Strauss, A., Frangopol, D.M. & Bergmeister, K. (eds) *Life-Cycle and Sustainability of Civil Infrastructure Systems: Proceedings of the Third International Symposium on Life-Cycle Civil Engineering (IALCCE 12)*, Vienna, 3–6 October, CRC Press, Boca Raton

Goldstein, R.M., Zebker, H.A. & Werner, C.L. 1988. Satellite radar interferometry: Two-dimensional phase unwrapping. *Radio Science*, 23, 713–720

Hill, N. & Stärk, A. 2015. Volume loss and long term settlement at Kempton Court, Whitechapel. In: Black, M., Dodge, C. & Yu, J. (eds) Crossrail Project: Infrastructure Design and Construction. ICE Publishing, London, 347–385

Hill, N. & Stärk, A. 2016. Long-term settlement following SCL-tunnel excavation. In: Black, M. (ed.) Crossrail Project: Infrastructure Design and Construction. ICE Publishing, London, 227–247

Hover, E., Psomas, S. & Eddie, C. 2015. Short- and long-term tunnelling induced settlements at Whitechapel Station. *Ground Engineering*, 30–40

Jurečič, N., Zdravković, L. & Jovičić, V. 2013. Predicting ground movements in London Clay. *Proceedings of the Institution of Civil Engineers – Geotechnical Engineering*, 166, 466–482

Lawrence, U., Menkiti, C. & Black, M.G. 2016. A regional scale groundwater monitoring programme for the Crossrail Project: strategy and implementation. In: Crossrail Project: Infrastructure Design and Construction. ICE Publishing, London, 417–430

Lawrence, U., Menkiti, C. & Black, M. 2018. Regional-scale groundwater investigations for the Crossrail project. *Quarterly Journal of Engineering Geology and Hydrogeology*, 51, 31–37

Lazecky, M., Perissin, D., Bakon, M., De Sousa, J.M., Hlavacova, I. & Real, N. 2015. Potential of satellite InSAR techniques for monitoring of bridge deformations. 2015 Joint Urban Remote Sensing Event, JURSE 2015, 4–7

Massonnet, D., Rossi, M., Carmona, C., Adragna, F., Peltzer, G., Feigl, K. & Rabaute, T. 1993. The displacement field of the Landers earthquake mapped by radar interferometry. *Nature*, 364, 138–142

Moreira, A., Prats-Iraola, P., Younis, M., Krieger, G., Hajnsek, I. & Papathanassiou, K.P. 2013. A tutorial on synthetic aperture radar. *IEEE Geoscience and Remote Sensing Magazine*, 1, 6–43

Osmanoğlu, B., Dixon, T.H., Wdowinski, S., Cabral-Cano, E. & Jiang, Y. 2011. Mexico City subsidence observed with persistent scatterer InSAR. *International Journal of Applied Earth Observation and Geoinformation*, 13, 1–12

Osmanoğlu, B., Sunar, F., Wdowinski, S. & Cabral-Cano, E. 2016. Time series analysis of InSAR data: Methods and trends. *ISPRS Journal of Photogrammetry and Remote Sensing*, 115, 90–102

Rosen, P.A., Hensley, S., Joughin, I.R., Li, F.K., Madsen, S.N., Rodriguez, E. & Goldstein, R.M. 2000. Synthetic aperture radar interferometry - Invited paper. *Proceedings of the IEEE*, 88, 333–382

Royse, K.R., de Freitas, M.H. et al. 2012. Geology of London, UK. *Proceedings of the Geologists' Association*, 123, 22–45

Wongsaraj, J., Soga, K. & Mair, R.J. 2007. Modelling of long-term ground response to tunnelling under St James's Park, London. *Géotechnique*, 57, 75–90

Wongsaraj, J., Soga, K. & Mair, R.J. 2013. Tunnelling-induced consolidation settlements in London Clay. *Géotechnique*, 63, 1103–1115